In Proceedings of "High Level Radioactive Waste Management Conference"
April, 1993 Las Vegas, NV USA

MODELING GRAVITY-DRIVEN FINGERING IN ROUGH-WALLED FRACTURES USING MODIFIED PERCOLATION THEORY

Robert J. Glass
Geosciences Center, Department 6115
Sandia National Laboratory
Albuquerque NM 87185
(505)844-0945

ABSTRACT

Pore scale invasion percolation theory is modified for imbibition of wetting fluids into fractures. The effects of gravity, local aperture field geometry, and local in-plane air/water interfacial curvature are included in the calculation of aperture filling potential which controls wetted structure growth within the fracture. The inclusion of gravity yields fingers oriented in the direction of the gravitational gradient. These fingers widen and tend to meander and branch more as the gravitational gradient decreases. In-plane interfacial curvature also greatly affects the wetted structure in both horizontal and non-horizontal fractures causing the formation of macroscopic wetting fronts. The modified percolation model is used to simulate imbibition into an analogue rough-walled fracture where both fingering and horizontal imbibition experiments were previously conducted. Comparison of numerical and experimental results showed reasonably good agreement. This process oriented physical and numerical modeling is a necessary step toward including gravity-driven fingering in models of flow and transport through unsaturated, fractured rock.

INTRODUCTION

Gravity-driven fingering in rough-walled, unsaturated fractures has been demonstrated and studied experimentally by Nicholl et al.[1,2,3] They explored the effects of boundary conditions, initial conditions and angle with respect to vertical in an analogue rough-walled fracture. In order to bound the occurrence and behavior of the phenomenon, we must understand the additional influence of aperture field (distribution, spatial structure and heterogeneity), contact angle, and matrix imbibition. For more general application, the effects of surface tension and density also must be considered. While systematic experimentation evaluating the aforementioned system parameters is necessary, numerical modeling is required to treat the myriad of parameter combinations expected in nature. Process oriented numerical modeling is also the first step toward including the fingering phenomenon in models of flow within large-scale, unsaturated, fractured rock systems. These phenomena may have significant impact on unsaturated groundwater flow at the proposed Yucca Mountain radioactive waste repository.

Here we introduce a conceptual model to simulate wetted structure including finger formation during imbibition into rough walled fractures at arbitrary angle in the gravity field. The model is a modified form of invasion percolation and thus applies in the quasi-static limit, i.e., for low flow conditions where fingers will be at a minimum size. In addition to gravity, the first order effects of local aperture geometry and curvature of the air/water interface in the plane of the fracture are also incorporated. This effect is required to produce macroscopic air/water interfaces (compact clusters) and macroscopic fingers as observed in experiments where a wetting fluid invades a fracture. Dynamic effects at higher flow rates as described by Nicholl et al.[1,2,3] are not addressed. Matrix effects currently are not included; the model simulates imbibition in fractures within impermeable media or under time scales or saturations where matrix effects are negligible.

We compare model prediction with experimental results for the transparent analogue rough-walled fracture used by Nicholl et al.[1,2,3] Horizontal imbibition, capillary rise (vertical), and downward infiltration as a function of angle relative to vertical were explored. In the downward infiltration situation, gravity driven fingers are predicted by the model and form in the experiment.

CONCEPTUAL MODEL DEVELOPMENT

Figure 1 shows a two image sequence of a downward growing finger in an initially dry, transparent analogue fracture (from the experiments of Nicholl et al.[2]). Analysis of images such as these shows that in initially dry fractures, finger tips are essentially short, locally saturated, water columns that partially drain along their trailing edge as they propagate downward. The length of the saturated zone, L_s, of all finger tips is found to be greater than the difference between air entry value and the water entry value of the hysteretic pressure potential/saturation relation. As flow rate to the finger increases, finger velocity, width and L_s increase; in the "high flow" limit a stable one-dimensional flow field is forced.[1] Thus, while gravity driven fingering is a highly dynamic process, these observations show that increasing viscous forces by increasing the system flow rate stabilizes the flow field. It should be noted that the converse is true for viscous-driven fingering.

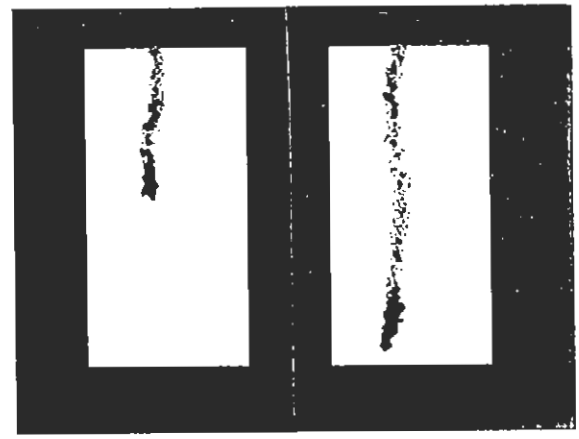

Figure 1: Sequence of images showing the downward growth of a finger generated from a low flow rate, single point source at the top of a transparent analogue fracture.

At the "low flow" limit where fingering will dominate the flow field, the dynamics are primarily confined to the front and back of the spanned aperture cluster constituting the finger tip. At these locations, localized flow occurs in jumps as the meniscus spanning an individual aperture becomes unstable and moves rapidly to fill an adjoining site or empty the aperture. Since finger growth is controlled primarily by this jump mechanism, an aperture scale model that incorporates only this mechanism may be appropriate. Under these conditions, capillarity and gravity will combine to dictate growth only by determining which aperture is filled next, i.e. has the lowest filling potential. For this situation, a form of invasion percolation should apply.

Invasion percolation:

Invasion percolation, introduced by Wilkinson and Willemsen[4] for application to flow in porous networks, models an imbibition process where the pressure potential within each fluid does not vary in space. This is a reasonable assumption in the limit of infinitesimal flow rate where viscous forces are negligible and the system is dominated by capillary (surface tension) and body (gravity) forces. Invasion percolation is essentially a simplified form of the pore-scale models developed in the petroleum engineering field.[5,6]

Invasion percolation is implemented numerically as follows. First, a pore network of given connectivity is generated with each pore given a probability of filling from a uniform probability distribution. Certain pores are then filled as the boundary wetting surface, often either an edge of a rectangular network or a disk at the center. All pores connected to the wetted pore surface are available for filling and the one with the highest assigned probability of filling is found and filled. This modifies the list of pores available for filling and the modified list is next sorted to find once again the pore with the highest assigned probability of filling and so on. Pores that become entrapped may or may not be removed from the pores available to be filled depending on the situation of interest. If the non-wetting fluid is incompressible or nearly so, then removal is appropriate. Conversely, if the non-wetting fluid is infinitely compressible or will dissolve in the wetting phase then entrapped pores should not be removed. The process is stopped when no pores are found that are above a specified cutoff in assigned probability of filling.

Invasion percolation has been shown to conform reasonably well to the invasion of a porous medium by a non-wetting fluid. Under these conditions the fluid-fluid interface exhibits structure on all scales down to the pore scale and has been shown to be fractal.[7] For wetting fluids invading porous networks or fractures as we have in our problem, interfaces are much smoother and saturation fronts characteristically form. Invasion percolation modified to include gravity and what was termed multiple-neck, pore filling "facilitation", was applied in the quasi-static limit to gravity-driven fingering in porous media by Glass and Yarrington.[8] Facilitation takes into account the first order effects of pore geometry beyond the usual assumption of circular or spherical pores. This effect causes the formation of macroscopic fingers instead of the pore scale fingers predicted from invasion percolation with gravity

alone. Here we extend this earlier work to fractures at arbitrary flow inclination by including gravity, local aperture dilation or convergence, and interfacial curvature in the plane of the fracture.

Modified Invasion Percolation:

The fracture aperture field is conceptualized as a planar checkerboard of individual elements. The center of each element has a known local aperture. To include gravity in proper magnitude relative to capillary forces, we cast the probability of filling in terms of a total aperture filling potential. This approach was first applied by Wilkinson[9] to study the effect of buoyant forces on the mixing region between two vertically stratified immiscible fluids in a porous medium. The total aperture filling potential, ψ_t, is calculated as the sum of the pressure and gravity potentials. Pressure potential, ψ_p, is a function of the two principal radii of interfacial curvature r_1 and r_2, the surface tension σ, the fluid density ρ, and the gravitational acceleration g, given by the Laplace-Young relation

$$\psi_p = \frac{-\sigma}{\rho g} (1/r_1 + 1/r_2) \qquad (1)$$

Gravity potential, ψ_g, is simply given by

$$\psi_g = - z \cos\delta \qquad (2)$$

where z is the spatial coordinate defined in the plane of the fracture to be positive into the aperture network from the invasion edge and δ is the angle between vertical and the plane of the network.

To apply equation (1) to a fracture we take one principal radius of curvature, r_1, to be normal to the plane of the fracture (given by half the local aperture) and the other, r_2, to be in the plane of the fracture (see figure 2). To account for wettability effects, we modify r_1 by the contact angle between the fracture surface, air and water given by α. In addition, we can take into account the local widening and narrowing of the local aperture as we move from point to point within the fracture. The dilation or convergence angle of the two fracture surfaces, β, is calculated to first order by fitting a straight line between known aperture points. Note that for widening aperture, β will be positive but for narrowing it will be negative. The effect of incorporating the local aperture geometry yields a local directional dependency of the aperture filling potential.

For a wetting fluid, in-plane curvature does not intersect the solid fracture surface and so only the geometry of the interface in the plane of the fracture need be known to calculate the local r_2. (In-plane curvature is illustrated in images of the fracture wetted structure shown in figures 6 through 9 for simulations and figure 11 for horizontal imbibition in a physical experiment.) While in principle r_2 may be calculated rigorously, the computational penalty is extreme. Here we approximate r_2 to first order by considering only the final configuration of the interface when the aperture location (node) is achieved, i.e., the aperture is spanned. This yields three conditions that can be easily evaluated by the number of adjacent aperture nodes filled with water (see figure 2b, c, and d). The first condition is a location that has only one adjacent filled aperture node; r_2 will be negative and equal to d, the distance between apertures. For two and three adjacent filled aperture nodes, the local interface will be nearly flat when the location is achieved and thus r_2 will add a negligible influence (i.e., r_2 is large). This simple implementation of in-plane curvature is expected to form compact clusters of spanned apertures and macroscopic fronts.

Incorporating the α, β, and the in-plane curvature into the total filling potential for a given aperture, ψ_t, we have our working equation

$$\psi_t = \frac{-\sigma}{\rho g} (\cos(\alpha+\beta)/r_1 - \gamma/d) - z \cos\delta \qquad (3)$$

where γ is a switch which is dependent on the number of adjacent filled apertures: equal to 1 for one adjacent filled aperture and zero for two and three.

This modified invasion percolation model is implemented numerically as follows: First, an aperture network with orthogonal, four-fold connectivity (checkerboard) is measured from a fracture or generated using a variety of models assuming a random or spatially correlated aperture field. Next, aperture filling potentials are calculated as given by equation (3). The apertures along the top of the aperture network are filled initially as the boundary wetting surface. All apertures connected to the wetted pore surface are available for filling and the one with the most negative filling potential is found and filled. This modifies the list of apertures available for filling and the in-plane curvature of the interface within the fracture. The filling potential of apertures available for filling are modified to account for the in-plane curvature and the list is next sorted to find once again the aperture with the most negative assigned filling potential and so on.

Currently, numerical experiments implement only the wetting-phase invasion component of the process. Inclusion of the drainage of apertures during a simulation, however, is a

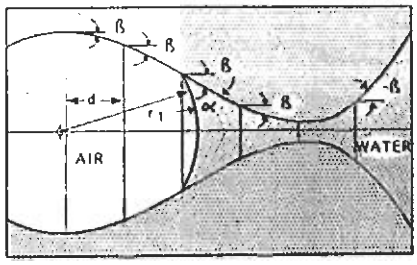

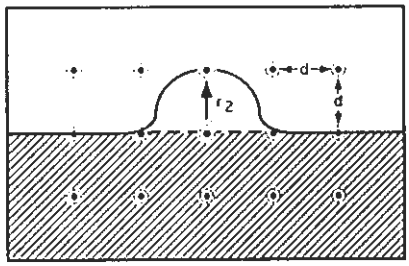

$r_2 = d$

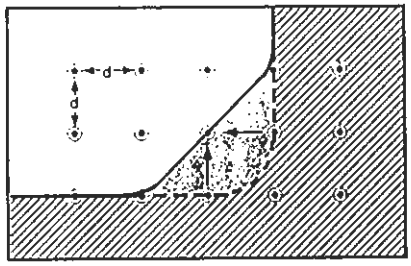

$r_2 \gg d$

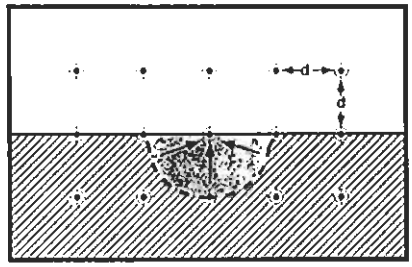

$r_2 \gg d$

Figure 2: Geometric arguments and definition of parameters. Drawings denote a) looking into the edge of a fracture with α, β, and r_1, b) looking down on the fracture plane, simplified in-plane curvature effect with one adjacent filled aperture, c) two adjacent filled apertures, and d) three adjacent filled apertures.

straightforward extension and should allow us to simulate both the penetration of the fracture by a finger tip and the drainage behind the finger tip.

MODEL BEHAVIOR AND COMPARISON TO EXPERIMENT

To evaluate model behavior we non-dimensionallze equation (3) so that the various effects can be weighed against one another. Choosing the characteristic length of the problem to be half the mean aperture, r_m, we have

$$\psi_c^* = - C \left(\cos(\alpha+\beta)/r_1^* - \gamma/d^*\right) - z^* \cos\delta \qquad (4)$$

where ψ_c^*, z^*, r_1^* and d^* are all given by their original values divided by r_m and C is the capillary-gravity ratio given by

$$C = \frac{\sigma}{\rho g r_m^2} \qquad (5)$$

C is simply a force ratio between surface tension and gravity. We see from equation (4) that given a particular fluid-fluid-surface combination the importance of gravity is inversely related to r_m^2.

The interplay between the two capillary terms within the parenthesis is complicated and depends on the details of the local aperture field. The first capillary term is influenced by variability in r_1^* and β, both of which will cause irregularity in the air/water interface. The contact angle, α, which we assume here to be a constant for the fracture, affects this term as a nonlinear scaling factor in its combination with β.

The second capillary term is a constant for a regular aperture network (or data grid), however whether γ is non-zero depends on the local interfacial curvature such that it provides a smoothing force. Choice of aperture network resolution defines d^* so that as network spatial resolution decreases, the importance of in-plane interfacial curvature decreases. Unless r_1^* smooths appropriately as resolution decreases, the choice of resolution scale will be critical in simulating wetted structure within the fracture plane.

As a first step in analyzing model behavior, we focus in the remainder of the paper on the effects of the in-plane curvature term, the gravity term and the aperture field determined β. These are the new and critical modifications to invasion percolation that allow us to model the wetted structure evolution during imbibition in fractures. We assess their effects within an aperture field measured from the analogue rough-walled fracture used by Nicholl et. al.[1,2,3] in their experiments on gravity driven fingers, and

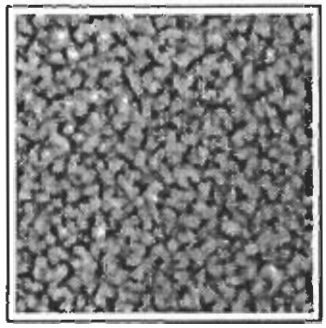

Figure 3: Grey scale image of profilometer aperture field. Field is 256 x 256 points over an area of 2.56 cm x 2.56 cm (see grey scale bar in figure 5).

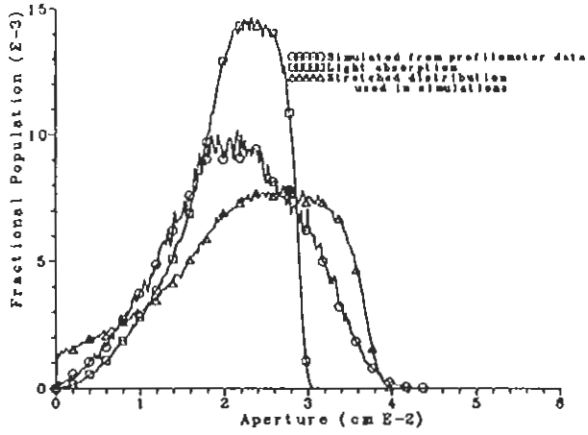

Figure 4: Histograms of aperture fields.

compare our simulations with their experimental observations.

Aperture field:

The analogue rough-walled fracture considered here was formed with commercially available "obscure" glass which had one rough surface. The rough surfaces of two pieces of the glass were held at close contact in a transparent test cell with pressurized air. The mean aperture was measured volumetrically to be .2146 mm. The spatial resolution for data collection was chosen to be well below the correlation length of the fracture aperture field and to be approximately that of r_m for the fracture (.1073mm). This sets the value of r_2^* in equation (4) to approximately one.

The aperture field was measured both with a laser profilometer and with light absorption techniques. Laser profilometor measurements were made of the manufactured glass surface at a grid of 256 x 256 points separated by .1 mm on one side (a 2.56 x 2.56 cm^2 area). The spatial resolution of the measurement was .007 mm, the diameter of the beam. An aperture field was numerically simulated by superimposing the topography of the glass surface over the same topography reversed and rotated 180 degrees. The distance between the two surfaces was adjusted to yield a mean separation equal to the measured mean aperture noted above. Figure 3 shows a grey scale image of the simulated aperture field. Geostatistical analysis showed the field to be isotropic with a correlation length of .7 mm. The histogram of the apertures is plotted in figure 4.

Because the profilometer data encompassed too small an area of fracture (2.56 cm x 2.56 cm) for our numerical experiments, a light absorption technique was used to obtain the aperture field on a large 10 cm x 20 cm section of the intact transparent analogue fracture. The fracture was filled first with a clear 135% sucrose solution which approximately matched the index of refraction for the glass plates. The clear sucrose solution was then replaced with an identical solution containing dye. Digital images (1024 x 2048 pixels) were taken at a resolution of .1 mm and processed using simple exponential light absorption theory to yield the aperture field. Analysis of this aperture field showed approximately the same correlation length as the simulated aperture field from the laser profilometer data, however, the distribution about the mean aperture was substantially narrower (see figure 4).

The discrepancy in the absolute value of the fracture aperture derived by the two techniques as depicted in the different aperture distributions is most likely due to differences in measurement scale. The sampling resolution of the two methods are over two orders of magnitude different, .01 mm^2 for the light transmission and .000049 mm^2 for the laser profilometer. Thus, while the light transmission technique captured the details of the aperture structure and connectivity extremely well, it yields aperture values that are smoothed about the mean. To account for this discrepancy while maintaining the mean aperture and structure of the field, the distribution was stretched to approximate the range that was simulated from the profilometer data (see figures 4 and 5). Standard and modified invasion percolation simulations conducted on this fracture aperture field and that of the profilometer were very comparable.

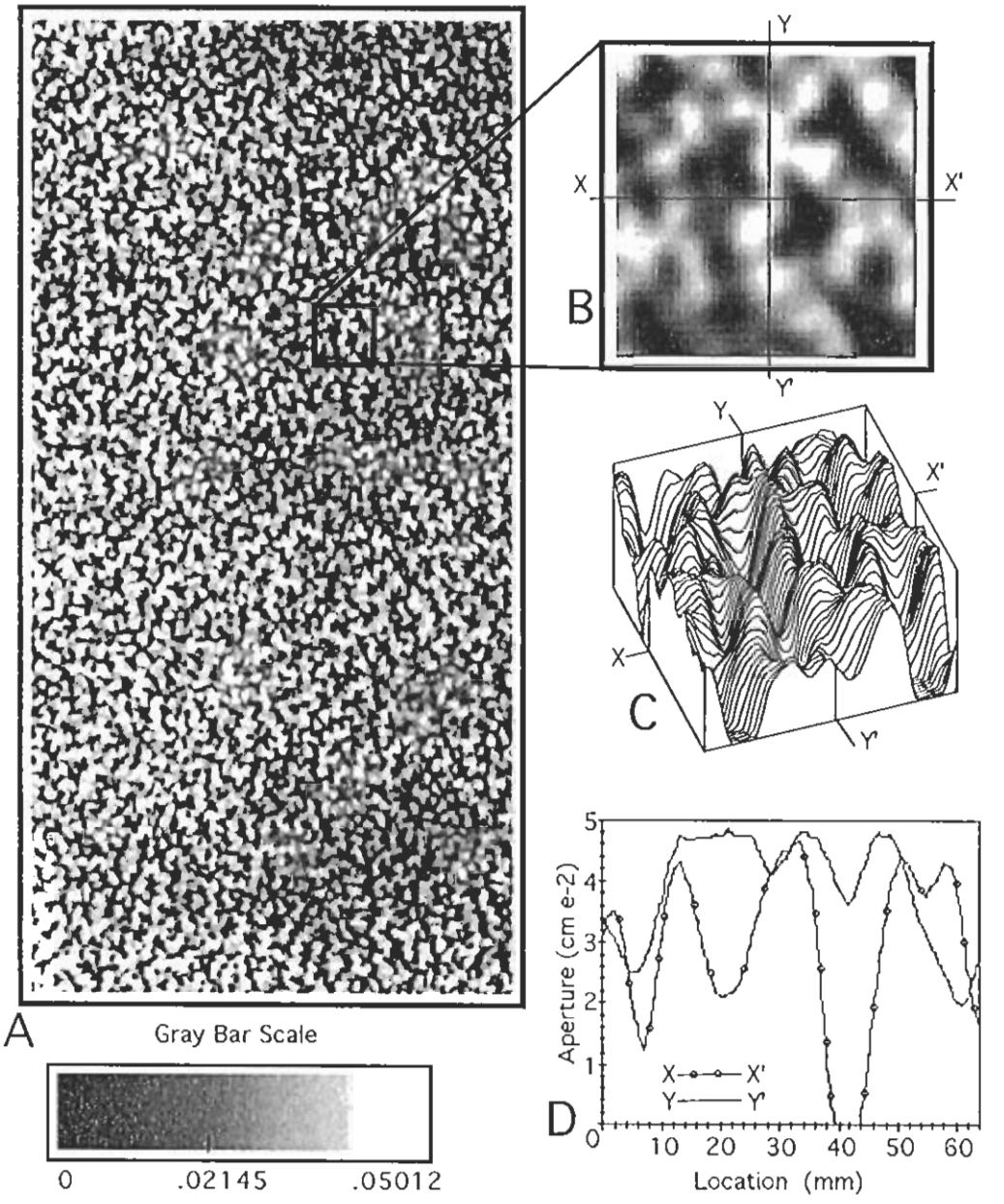

Figure 5: Aperture field used in numerical simulations: a) Grey scale image of 512 x 1024 (5.12 cm x 10.24 cm) aperture field measured by light absorption methods with distribution stretched to yield maximum and minimum values consistent with the profilometer. Aperture field mean and structure are preserved. b) grey scale blow up of a small 64 x 64 region of the field. c) three-dimensional plot of the small region in b. d) x and y transect of the small region in b and c.

Numerical experiments:

A matrix of numerical experiments with β either included or set to zero and in-plane curvature either included or not (γ set to zero), were carried out for gravitational gradients ($\cos(\delta)$) of 1, .75, .5, .25, 0 and -1. The first four correspond to downward imbibition at angles with respect to vertical of 0, 41.4, 60 and 75.5 degrees respectively. The fifth and sixth correspond to horizontal and capillary rise (vertical upward) imbibition, respectively. For all simulations the contact angle was held at 35 degrees, the approximate value determined from visual inspection of a drop of fluid placed on the glass plate. The surface tension and density were also held constant at their standard temperature and pressure values. The top center 512 x 1024 pixel portion (5.12 cm x 10.24 cm) of the 1024 x 2048 pixel fracture aperture field was used for simulation. Air was treated as incompressable by implementing a trapping algorithm. Constant pressure boundary conditions were imposed for the air phase on the bottom and each side of the aperture field. To begin the simulation, the top row of apertures was filled with water and the percolation process started. Simulation was stopped when either the end of the aperture field was reached or zero potential within the network was reached (for capillary rise experiments).

Results:

The wetted structure when water first reaches the other side of the aperture field (breakthrough) for each of the simulations is shown in figures 6 through 9. Each figure consists of simulations run at angles with respect to vertical of 0, 41.4, 60, 75.5, 0 (horizontal) and 180 (vertical). Figure 6 describes the baseline case of standard invasion percolation and subsequent figures display the effects of the modifications to invasion percolation introduced here. Black regions denote locations where water spans the aperture, grey regions where air has become entrapped and white where the air phase is present and connected to a boundary where it can escape.

Gravity: Gravity acting downward causes the formation of fingers in all cases. As the angle with respect to vertical increases from 0 (vertical downward) to 90 degrees (horizontal), fingers widen and become more complicated, i.e., more meandering and branching. This can also be seen in equation (4); as gravity becomes less important with respect to aperture field variability, complication of the front will increase. Uniform propagation direction of the fingers (downward) decreases as the angle increases so that in the horizontal case, fingers have no preferred direction and often curl back on themselves. This behavior is referred to as capillary fingering and is completely determined by the aperture field. When it is isotropic as we have in our fracture aperture field, capillary fingers will span the network from side to side before spanning the network from top to bottom. Finger width measured normal to the network side for angles below 90 degrees is plotted as a function of gravitational gradient in figure 10. Capillary rise is shown in the f part of figures 6 through 9. Gravity significantly depresses capillary fingering during capillary rise.

In-plane curvature: The effect of in-plane curvature is dramatic. When it is not included (figs 6 and 7) the wetted aperture field follows the network of small apertures and entraps air in the large apertures. The complication of the wetted structure is similar to the complication of the fracture aperture field. Application of invasion percolation to a random network yields complication down to the grid scale.[4] Since we have a spatially correlated field, the complication only extends down to or slightly above the correlation length. When in-plane curvature is included (figs 8 and 9), macroscopic fronts well above the correlation length form and entrapped air decreases dramatically. In-plane curvature also decreases the capillary rise in the fracture. Using the mean aperture (.02146 cm), rise between two parallel plates at a contact angle of 35 degrees should be 5.7 cm. This is roughly the rise when in-plane curvature is not included. Rise in the fracture when in-plane curvature is included, however, is 3.2 cm, a depression of almost 50%. This can be understood with reference to equation (4) since in-plane curvature acts to increase the filling potential (make less negative).

β: The effect of convergence and dilation of the local aperture field is seen to be small in terms of the general behavior of the model. The wetted structures with (figures 7 and 9) and without (figures 6 and 8) β look similar, however, the exact structure is different. This difference is due to the fact that β slightly modifies the aperture hierarchy within the field. For other aperture fields or larger contact angles this may not be the case and β may significantly influence gross wetted structure.

Comparison to experiment:

Figure 11a shows the wetted structure at breakthrough for a horizontal imbibition test during the experiments of Nicholl et al.[1,2,3] The scale of the experiment is double that of the numerical simulation in both length and width. The compact structure of the wetting front is comparable to that in the simulations which included in-plane curvature (figures 8 and 9), however the simulated structure is a bit "blockier".

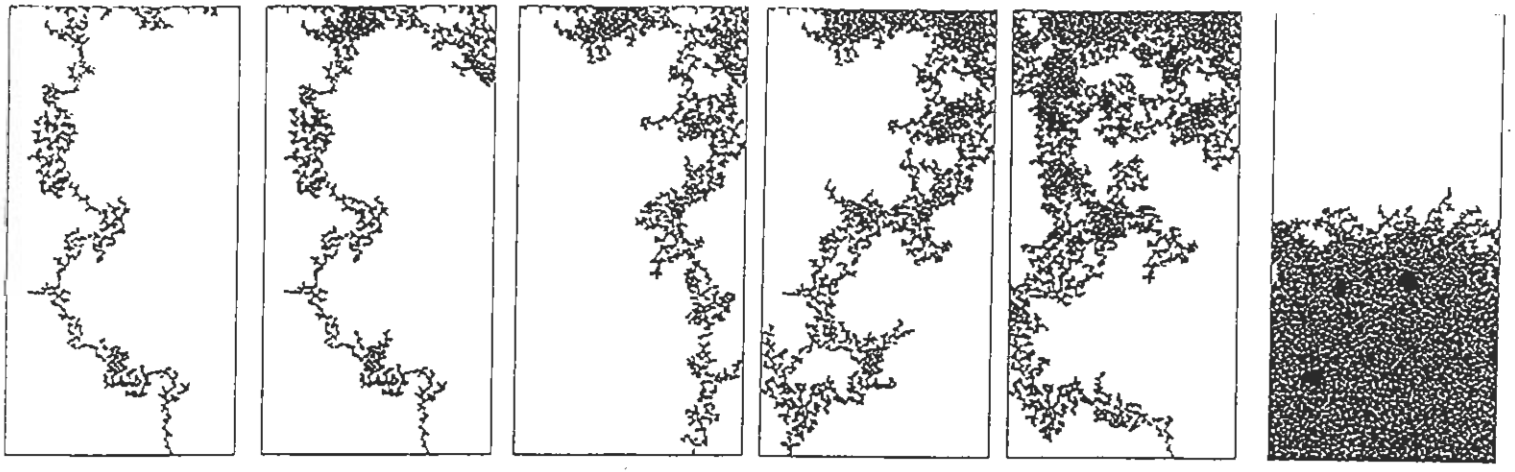

Figure 6: In-plane curvature not included, β set to zero (standard invasion percolation): Wetted structure is shown at breakthrough. Black regions are clusters of wetted aperture, grey denotes regions of air entrapment, and white regions contain air that is connected to a boundary and can escape. Angles (in degrees) with respect to vertical downward are a) 0, b) 41.5, c) 60, d) 75.5, e) 90 (horizontal), f) 180 (capillary rise, vertical downward). Water enters the aperture field from the top of the network in a) through e) and from bottom in f).

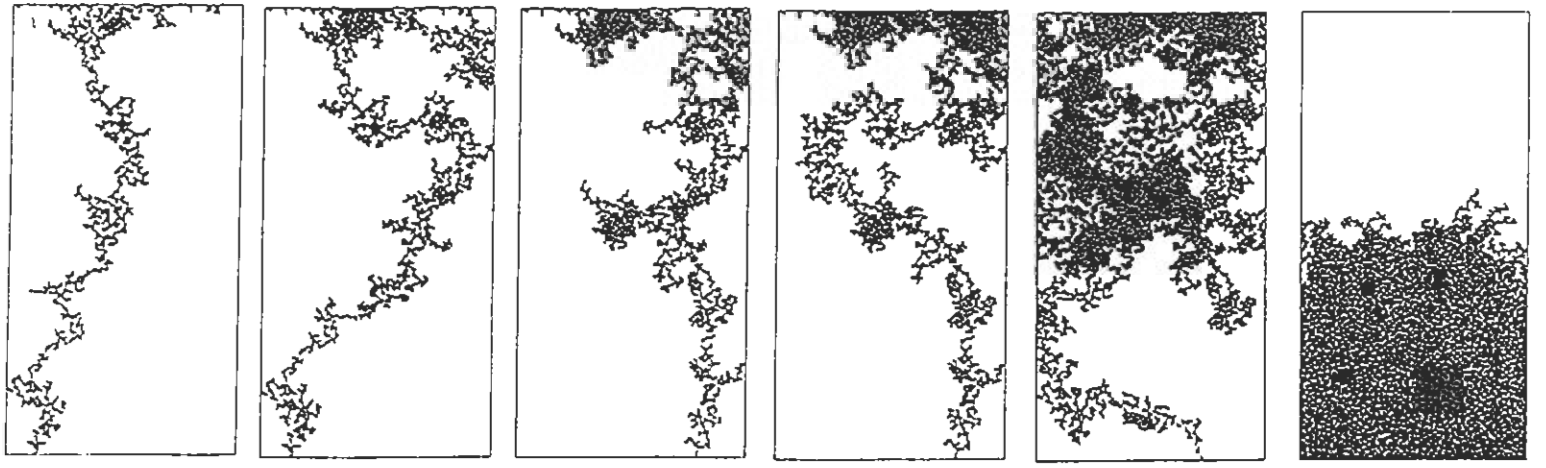

Figure 7: In-plane curvature not included, β calculated: Wetted structure is shown at breakthrough. See figure 6 caption for further details.

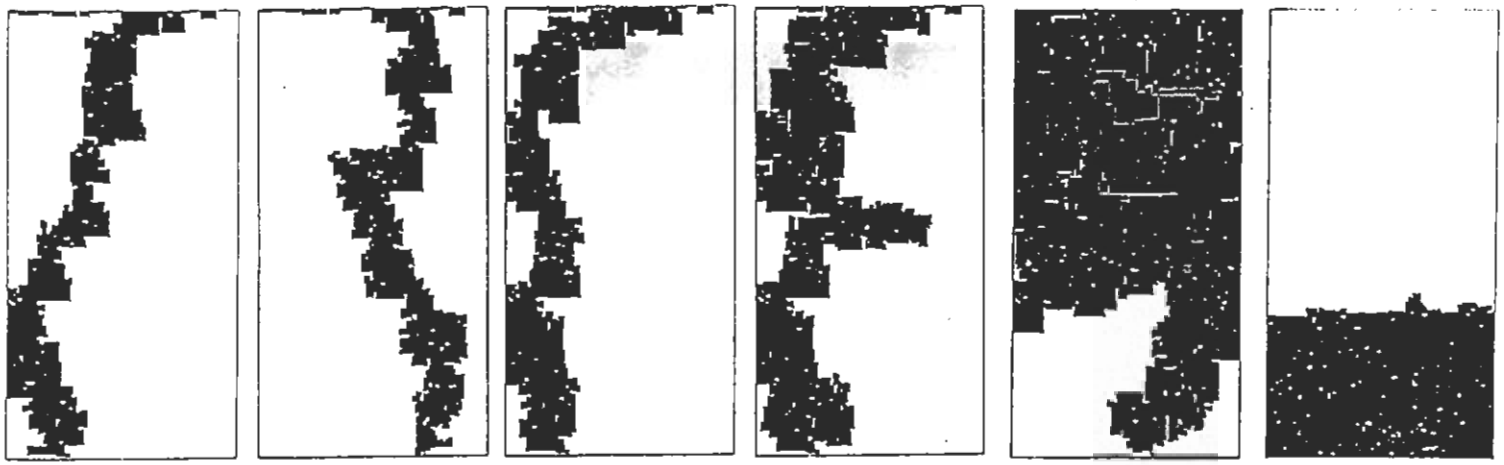

Figure 8: In-plane curvature included, β set to zero: Wetted structure is shown at breakthrough. See figure 6 caption for further details.

Figure 9: In-plane curvature included, β set to zero: Wetted structure is shown at breakthrough. See figure 6 caption for further details.

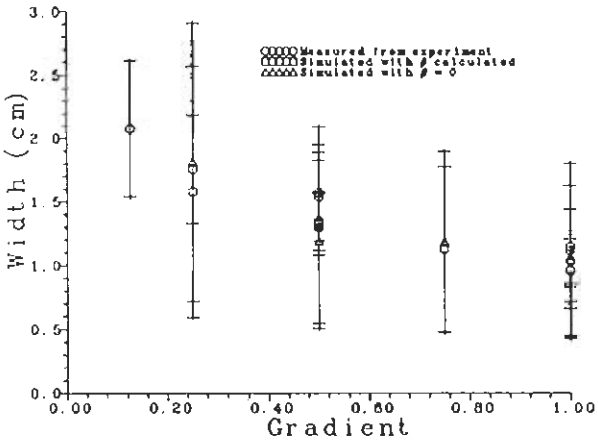

Figure 10: Finger width and standard deviation for numerical simulations and physical experiment as function of gravitational gradient. Widths are measured normal to the side of the aperture field (in the direction of the gravitational gradient).

Capillary rise height in the fracture was measured in over 100 experiments, yielding a value of 2.25 +-0.26 cm. Capillary rise in our vertical imbibition simulations with in-plane curvature included was greater by almost fifty percent. Several possible explanations exist for this discrepancy. As mentioned by Nicholl et al.[2] they measured the capillary rise at the bottom edge of their fracture and the measurement may not be free of edge effect. It is also possible that the contact angle for the fracture is greater than we estimated by eye. Planned studies using digital imaging to determine the dynamic contact angle will yield a better estimate of α.

Outlines of fingers recorded digitally during experiments that generated single fingers from a point source located at the top of the fracture are shown in figure 11b, c, and d. Note that the width and length scales of these images are double that of the numerical experiments. Flow rates for all the fingers were approximately .025 ml/min, the lowest stable flow rate that could be maintained by the pump. Angle with respect to vertical is noted in the caption and the average finger width +- std for the fingers is plotted in figure 10 along with the simulated finger widths. Both the qualitative and quantitative aspects of the finger structure are reasonably well simulated by the modified invasion percolation model when in-plane curvature is included. Again, simulations do tend to be more blocky than the experimental wetted structures due to the rectangular nature of the grid.

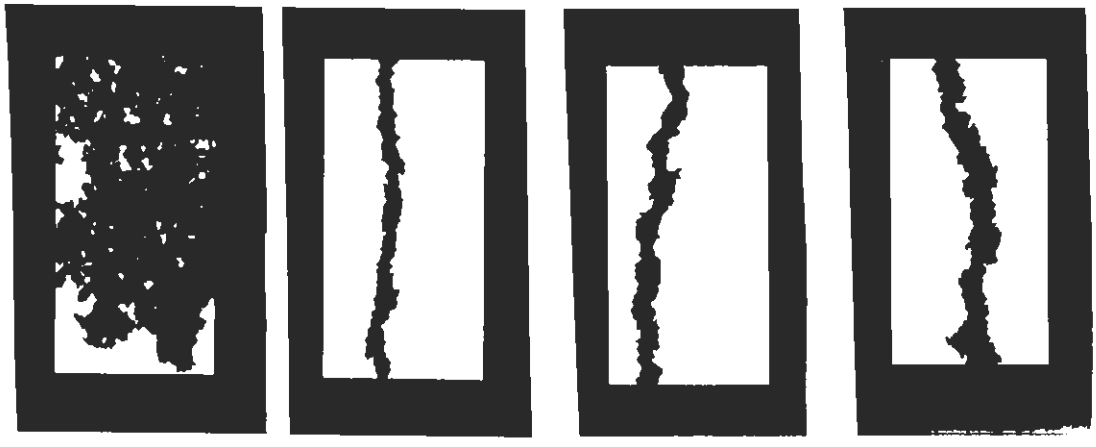

Figure 11: Wetted structure for imbibition tests in analogue rough-walled fracture. a) at breakthrough for a horizontal imbibition test and b) 0 degrees (vertical downward), b) 60 degrees, and c) 75.5 degrees with resepect to vertical downward. Spatial scale is two times wider and longer than the numerical simulations.

CONCLUSIONS

The modified invasion percolation model introduced here simulates wetted structure within fractures at arbitrery angle with respect to vertical. Comparison to experimental data shows good agreement. The inclusion of gravity yields fingers oriented in the direction of the gravitational gradient. These fingers widen and tend to meander and branch more as the gravitational gradient decreases. Details of the convergence and divergence of the local aperture field have only a second order effect on wetted structure in the aperture field we studiad. In-plane interfacial curvature, however, greatly affects the wetted structure in both horizontal and non-horizontal fractures. This piece of physics, which is lacking in standard percolation modeling approaches, causes the formation of macroscopic fronts analogous to real wetting fronts observed in wetting fluid invasion in fractures. Fronts are thus not simply a dynamic effect.

Non-dimensionalization of the total filling potential equation suggests model and physical systems to behave as follows. Aperture variability (including β), gravity, and in-plane interfacial curvature all compete to determine filled aperture structure. Choices of values of the parameters describing each can be made such that one dominates over the others. Where gravity dominates, fingers move through the network. Where in-plene interfacial curvature dominates, water moves across the network from the supply surface with one macroscopic front. Where aperture variability dominates, the structure conforms to standard invasion percolation. A series of physical experiments and numerical sensitivity studies are required to document and characterize this expected behavior. This process oriented physicel and numerical modeling is a necessary step toward including gravity-driven fingering in models of large-scale, unsaturated, fractured flow systems.

ACKNOWLEDGEMENTS

The author gratefully acknowledges the assistance and support of the following: Sharon Shannon who wrote several wetted structure analysis programs; Lane Yarrington who programmed the trapping algorithms incorporated in the model and several wetted structure visualization programs; Mike Nicholl who provided discussion and along with Mike Wilson, carefully reviewed the paper; and Steve Brown, Craig Ginn, Chris Rautman and Huy Nguyen who helped measure, analyze and visualize the aperture fields. This work was supported by the U.S. Department of Energy, Office of Civilian Radioactive Waste Management, Yucca Mountain Site Characterization Project Office, under contract DE-AC04-76DP00789.

REFERENCES

1. M.J NICHOLL, R.J. GLASS, and H.A. NGUYEN, "Gravity-driven fingering in unsaturated fractures". Proc. 3rd Int. Conf. of High Level Rad. Waste Manage., Las Vegas, Nevada, April 12-16 (1992).

2. M.J. NICHOLL, R.J. GLASS, and H.A. NGUYEN, "Small-scale behavior of single fingera in an initially dry fracture", Proc. 4th Int. Conf. of High Level Rad. Waste Manage. Las Vegas, Nevada, April 26-30 (1993).

3. M.J. NICHOLL, R.J. GLASS, and H.A. NGUYEN, "Wetting front instability in initially wet fractures", Proc. 4th Int. Conf. of High Level Rad. Waste Manage., Las Vegas, Nevada, April 26-30 (1993).

4. D. WILKINSON and J.F. WILLEMSEN, "Invasion percolation: a new form of percolation theory. J. Phys. A:Math. Gen. 16:3365-3376 (1983).

5. I. FATT, "The Network Model of Porous Media I. Capillary Pressure Characteristics," Petroleum Transactions, AIME, 207, 144-159 (1956).

6. I. CHATZIS and F.A.L. DULLIEN, "Modelling Pore Structure by 2-D and 3-D Networks with Application to Sandstones," Technology, Jan-March, 97-108 (1977).

7. R. LENORMAND, C. ZARCONE "Invasion percolation in an Etched Network: measurement of a fractal dimension", Phys. Rev. Lett. 54:2226-2229 (1985).

8. R.J. GLASS and L. YARRINGTON, "Analysis of wetting front instability using modified invasion percolation theory", EOS, 70:1117 (1989).

9. D. WILKINSON, "Percolation model of immiscible displacement in the presence of buoyancy forces", Phys. Rev. A. 30:520-531 (1984).